Multiplicity and stability of travelling wave solutions in a free boundary combustion-radiation problem

Baconneau, O.; van den Berg, G.J.B.; Brauner, C.-M.; Hulshof, J.

published in
European Journal of Applied Mathematics
2004

DOI (link to publisher)
10.1017/S0956792503005333

document version
Publisher's PDF, also known as Version of record

Euro. Jnl of Applied Mathematics (2004), *vol.* 15, *pp.* 79–102.
DOI: 10.1017/S0956792503005333 Printed in the United Kingdom

Multiplicity and stability of travelling wave solutions in a free boundary combustion-radiation problem

OLIVIER BACONNEAU[1], JAN BOUWE VAN DEN BERG[2], CLAUDE-MICHEL BRAUNER[1] and JOSEPHUU HULSHOF[2]

[1]*Université Bordeaux I, Mathématiques Appliquées de Bordeaux, 33405 Talence Cedex, France*
email: brauner@math.u-bordeaux.fr
[2]*Department of Mathematics, Vrije Universiteit Amsterdam, De Boelelaan 1081, 1081 HV Amsterdam, The Netherlands*
email: {janbouwe,jhulshof}@few.vu.nl

(*Received 31 April 2002; revised 15 August 2003*)

We study travelling wave solutions of a one-dimensional two-phase Free Boundary Problem, which models premixed flames propagating in a gaseous mixture with dust. The model combines diffusion of mass and temperature with reaction at the flame front, the reaction rate being temperature dependent. The radiative effects due to the presence of dust account for the divergence of the radiative flux entering the equation for temperature. This flux is modelled by the Eddington equation. In an appropriate limit the divergence of the flux takes the form of a nonlinear heat loss term. The resulting reduced model is able to capture a hysteresis effect that appears if the amount of fuel in front of the flame, or equivalently, the adiabatic temperature is taken as a *control* parameter.

1 Introduction

In this paper, we study travelling wave solutions of a one-dimensional two-phase Free Boundary Problem (FBP), which arises in the context of thermo-diffusive models for premixed flames propagating in gaseous mixtures of fuel and dust. We formulate the model, determine the travelling wave solutions and study their stability. The problem is a limiting case of a more general formulation studied in Brauner *et al.* (2001) (see also Buckmaster & Jackson (1994), Blouquin (1996) and Blouquin *et al.* (1997)). Although greatly simplified from a physical point of view, the limiting problem has many relevant features of the full problem, and its simplicity facilitates the analysis.

Before writing down the equations, let us first introduce the important physical parameters governing the model. The model contains the amount of fuel in the fresh region far ahead of the flame, y^-, as a control parameter. The temperature θ^- far ahead of the flame is considered to be fixed.

The *flame temperature* is denoted by θ^*. It determines the reaction rate $F(\theta^*)$, a modified Arrhenius law, which may have an ignition temperature θ_{ig} below, which it is zero.

For travelling waves, global conservation implies that the temperature far behind the flame is given by

$$\theta^+ = \theta^- + y^-. \tag{1.1.1}$$

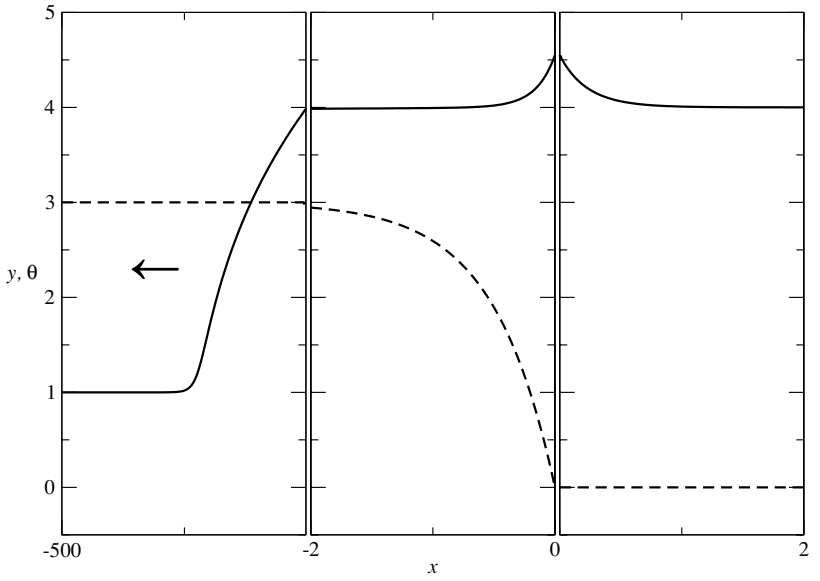

FIGURE 1. A travelling wave profile for the full problem with a radiative preheat zone far ahead of the flame. The solid line is the temperature profile, the dashed line is the fuel profile. Scales have been adjusted on the left. The profile is for $\alpha = 0.1, \chi = 0.1$, see Section 2, has $\theta^- = 1, y^- = 3, \theta^+ = 4$, and is moving with speed $\mu = 2$ to the left.

This θ^+ is called the *adiabatic* temperature: without radiation it would be the uniform temperature in the burnt region behind the flame. Radiative flames are characterised by a temperature overshoot at the flame front, which also enhances the flame velocity (the Joulin effect – see Buckmaster & Jackson (1994)).

The region ahead of the flame can be divided into a radiative preheat zone where the temperature is lower than θ^+, and a conductive preheat zone where the temperature is higher than θ^+. In the limit problem formulation below, the radiative preheat zone has disappeared from the problem formulation, as indicated in Figure 1. The limit problem, which we derive from the full problem in § 2, is formulated for the temperature $\Theta(x,t)$ and fuel mass fraction $Y(x,t)$ as functions of position x and time t, and for the flame front $x = s(t)$. It reads

$$Y_t = Y_{xx}, \quad x < s(t), \tag{1.1.2}$$

$$\Theta_t = \Theta_{xx} + \chi(f(\theta^+) - f(\Theta)), \quad x \neq s(t), \tag{1.1.3}$$

with the jump/boundary conditions

$$Y = [\Theta] = 0; \quad -Y_x = -[\Theta_x] = F(\Theta), \quad x = s(t), \tag{1.1.4}$$

expressing that the mass flux going into the flame balances the heat flux coming out of the flame, and is given by the reaction rate $F(\Theta)$. The parameter $\chi > 0$ acts as a heat loss parameter, a combination of the opacity and the ratio between convective and radiative fluxes (see § 2). Note that we have taken the diffusivities of Y and Θ to be the same, i.e. the Lewis number is equal to one (Le = 1).

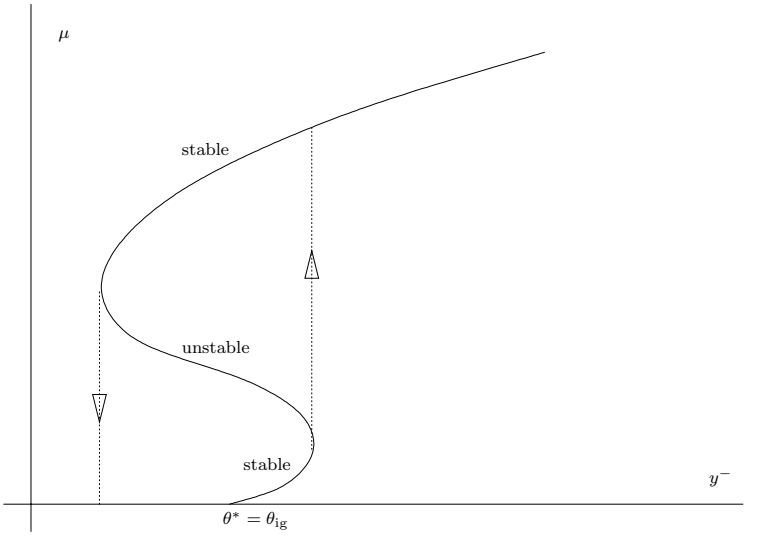

FIGURE 2. Travelling wave diagram in the (y^-, μ)-plane showing a hysteresis loop. The curve is parametrised by θ^*.

The radiative effects enter the equation for temperature through the nonlinear term $f(\Theta) - f(\theta^+)$, which is nothing but the divergence of the radiative flux. Here

$$f(\Theta) = \Theta^4. \tag{1.1.5}$$

This formulation is reminiscent of the modelling of premixed flames with radiative heat losses (see Buckmaster & Ludford (1982, p. 43) and Williams (1994, p. 271)), where one would have a formulation with a nonlinear term $f(\Theta) - f(\theta^-)$ in the temperature equation: radiative heat transfer may be compared to heat losses to a reservoir held at the adiabatic temperature.

Let us summarise the main results derived in this paper. We shall see in § 3 that travelling waves

$$Y(x,t) = y(x + \mu t), \quad \Theta(x,t) = \theta(x + \mu t),$$

where $\mu > 0$ is the flame speed, are completely characterised by the flame temperature θ^*. More precisely, we characterise such waves by a smooth curve $\theta^* \to (y^-(\theta^*), \mu(\theta^*))$ in the (y^-, μ)-plane, parametrised by θ^*. It is no restriction to assume that the travelling wave profiles have their front at $x = 0$, so $\theta^* = \theta(0)$. We present numerical calculations bearing evidence that the same is true for the full model.

The relation between y^- and θ^* is in general not bijective. The physical interpretation is that this leads to a hysteresis effect illustrated in Figure 2, where the control parameter y^- is on the horizontal axis, the propagation speed μ is on the vertical axis, and the flame temperature θ^* parametrises the solution curve. Note that at the starting point of the curve $\theta^+ = \theta^* = \theta_{ig}$ and $\mu = 0$.

We show that Figure 2 is illustrative: whether the curve moves to the left or to the right in the (y^-, μ)-plane depends on the size of $F'(\theta^*)$, the derivative of the reaction

rate $F(\theta^*)$ with respect to the flame temperature θ^*. We note that, from a mathematical point of view, $F'(\theta^*)$ may be interpreted as a *parameter* independent of $F(\theta^*)$. If it is smaller (larger) than a number which only depends on θ^*, y^- and μ, the curve moves to the right (left) as θ^* is increased. This interesting feature of possible multiple travelling wave solutions for the same value of the control parameter was already observed in the modelling literature, see [15]. In particular it is noteworthy that flames may exist with $\theta^+ < \theta_{ig} < \theta^*$, i.e. the adiabatic temperature may be below the ignition temperature. This is only possible because of the radiative effects taken into account by this model.

In §4 we shall argue that (orbital) *stability* is decided by the same criterium as above: if the curve $(y^-(\theta^*), \mu(\theta^*))$ moves to the right (left) as θ^* increases, the corresponding travelling wave solution is stable (unstable). Increasing y^-, a stable flame loses its stability as the solution branch in the (y^-, μ)-plane folds back (turns around). This causes the flame to jump to another travelling wave with a much larger flame temperature. If, after this threshold for y^- has been passed, y^- decreases, then the solution branch does not see the earlier threshold and may be continued until another turning point is reached, below which there are no travelling waves, and the flame disappears and extinction occurs (as indicated in Figure 2).

This is based on a linearisation technique for FBPs with jump conditions (see Brauner *et al.* (2000) and the references therein). The novelty of this technique is that it produces a linearised problem directly for the free boundary problem itself, rather than taking the limit of linearised problems in the high activation limit, as is done in [21]. As usual, the linear stability analysis leads to what is now commonly called an Evans function, its zeros being the eigenvalues of the linearised problem (Evans, 1975). In the travelling wave context in Terman (1990), the Evans function for the FBP would be the zero order term in Evans' function for the approximating problems (see also Balmforth *et al.* (1999)), and takes a simple form.

The functional analytic framework for this linearisation will be developed elsewhere. Here we only discuss the Evans function $D(\lambda)$ related to the linearised equations. The eigenvalues of the linearised operator are zeros of this function. Because of translation invariance, $D(0) = 0$, and the zero eigenvector is the spatial derivative of the travelling wave profile

$$\phi = \begin{pmatrix} y' \\ \theta' \end{pmatrix}.$$

We show that

$$D'(0) = 0 \iff \frac{dy^-}{d\theta^*} = 0,$$

a necessary condition for having a turning point. The sign of $D''(0)$ determines in which direction a real eigenvalue is passing through zero in a turning point.

Unfortunately there is no nice formula for $D''(0)$. The main difficulty here is not the nonlinear nature of the free boundary conditions but the nonlinearity of the function $f(\theta)$. In fact, we do give an explicit formula for $D(\lambda)$ in the special case that $f(\theta)$ is linear (i.e. $4 = 1$ in (1.1.5)), a model for conductive heat loss, which was also considered in Buckmaster & Jackson (1994). From this formula, we infer that there is at most one other eigenvalue except zero. This eigenvalue passes through zero in a turning point. It becomes positive (unstable flame) on the branch where $\frac{dy^-}{d\theta^*} < 0$ and it stays positive as long as,

increasing θ^*, the curve moves to the left. On the other branch it becomes negative (stable flame), and as long as where $\frac{dy^-}{d\theta^*} > 0$ it stays negative or becomes hidden in another sheet of the Riemann surface for $D(\lambda)$. So in the case of linear f, the picture is rather complete. Using numerical calculations again we find strong evidence that with f given by (1.1.5) the picture is exactly the same.

2 The model

Without radiation, the model presented below is the equidiffusional model for premixed flames (low Mach number, constant pressure and density, simple chemistry, planar flame), which gives the usual adiabatic flames.

The full radiative model (e.g. see Buckmaster & Jackson (1994)) consists of linear diffusion equations for the mass fraction Y of the fuel and the temperature Θ. In dimension one, these are simply

$$Y_t = Y_{xx}, \quad x < s(t), \tag{2.2.1}$$

$$\Theta_t = \Theta_{xx} - \beta q_x, \quad x \neq s(t), \tag{2.2.2}$$

where the radiative flux q in (2.2.2) is given by the Eddington equation

$$-q_{xx} + 3\alpha^2 q = -\alpha(\Theta^4)_x. \tag{2.2.3}$$

The radiative parameters are the opacity α and the Boltzmann number β. In (2.2.2) the divergence of the radiative flux appears with a minus sign.

As is quite common in thermo-diffusive models, the model in Buckmaster & Jackson (1994) is formulated as a free boundary problem, the thin reaction zone being replaced by a free boundary $x = s(t)$, the flame front, where the reaction takes place (see also Sivashinsky (1977) and Fife (1988)). This is expressed by the jump conditions

$$Y = [\Theta] = 0; \quad -Y_x = -[\Theta_x] = F(\Theta), \quad x = s(t). \tag{2.2.4}$$

The brackets denote the jump at $x = s(t)$, i.e. the difference of the spatial limits taken from the right and from the left, of the quantity in between. The problem has to be solved for given initial conditions of the unknowns $\Theta(x,t)$, $Y(x,t)$ and $s(t)$. Behind the flame front, i.e. in the burnt region $x > s(t)$, the mass fraction is assumed to be zero.

The nonlinear function $F(\Theta)$ models the reaction rate at the flame front. It is assumed to be bounded and increasing for $\Theta > \theta_{ig}$, zero for $\Theta < \theta_{ig}$, and smooth, except possibly at the ignition temperature $\Theta = \theta_{ig}$. Typically, it is a modification of the Arrhenius law, see (3.3.20) in § 3.6. It manifests itself in the jump conditions for Θ_x and Y_x: the heat flux coming out of the flame balances the mass flux going into the flame and is determined by the value of $F(\Theta)$ at $x = s(t)$.

The Eddington equation, a well known approximation to the radiative field in astrophysics, can also be derived from the equation for the radiative intensity as a function of position, time, frequency and direction using the moment approximation (see Levermore (1996) to get an averaged flux which only depends on position and time (Dubroca & Feugeas, 1999, 2000). The closure assumption necessary for this approach is known as the

$P1$-model, and is valid close to radiative equilibrium. This relates the (averaged) radiative energy to Θ^4 and leads to a hyperbolic system for the radiative energy and flux. The time derivatives in this system may be neglected because photons travel with light speed and the reduced system amounts to (2.2.3). The parameter α is the (dimensionless) opacity, the reciprocal of the mean free path of a photon.

The modelling assumptions involve limiting values for Y at $x = -\infty$ and Θ at $x = \pm\infty$: y^-, θ^- and θ^+. It is quite common to put these limiting values as boundary conditions at infinity, especially in the travelling wave context in which problems are often formulated. Strictly speaking, though, they are either the limits of the initial data, and as such preserved by the solutions of the equations, as is the case for y^- and θ^-, or the limit of the (travelling wave) solution to which the solution converges. For travelling waves, global conservation implies that $\theta^+ = \theta^- + y^-$. The limit at $+\infty$ of the initial data for Θ is left behind by the solution as it develops its travelling wave profile.

Thus the control parameter isy_-, the amount of fuel far ahead of the flame. Of course we may just as well consider θ^+ as the control parameter and in the limit case presented below it will be convenient, and not too confusing for the reader to do so. We showed that, no matter what the values of the positive parameters θ^-, θ^+, α and β are, there is always a travelling wave solution if we assume that the reaction rate F is positive, increasing, continuous and bounded as a function of temperature (Brauner *et al.*, 2000). The travelling wave speed μ satisfies

$$\mu y^- = F(\theta^*).$$

A key feature to note is that the front temperature θ^* is larger than θ^+, and thereby also the speed μ is larger than the adiabatic speed $\mu_{\mathrm{ad}} = F(\theta^+)/y^-$. This effect may be quite significant (Joulin & Eudier, 1988). Without radiation the temperature in the burnt region is identically equal to θ^+. This is why θ^+ is called the adiabatic temperature, which is the temperature behind an adiabatic flame. In fact, the adiabatic temperature may very well be below the ignition temperature.

The existence result in Brauner *et al.* (2001) relies on Schauder's Fixed Point Theorem, and does not give any information about multiplicity of solutions or a global bifurcation picture. This lack of information is the main reason for considering limit cases and an interesting (and illuminating) one was introduced in Brauner *et al.* (2001). It corresponds to

$$\alpha\beta = \chi > 0, \quad \alpha \to 0. \tag{2.2.5}$$

In Brauner *et al.* (2001), we showed for travelling waves that in this limit the conductive preheat zone in front of the flame where the temperature is above the adiabatic temperature, extends to $x = -\infty$ (i.e. the radiative preheat zone vanishes). This is why we are led to formulate the limit problem for temperature profiles satisfying $\Theta \to \theta^+$ as $x \to \infty$ *and* as $x \to -\infty$ (cf. Figure 1). Note that multiplying (2.2.2) by β and invoking (2.2.5), one arrives at

$$\Theta_t = \Theta_{xx} + C - \chi\Theta^4.$$

The only plausible choice for the constant is $C = \chi(\theta^+)^4$ and therefore the limit evolution

problem is formulated with

$$\Theta_t = \Theta_{xx} + \chi(f(\theta^+) - f(\Theta)), \quad x \neq s(t), \tag{2.2.6}$$

where f is given by (1.1.5). Thus θ^- disappears behind the horizon as far as the temperature profile is concerned. It remains present though through (1.1.1) in (2.2.6).

Summarising, the limit model studied in this paper is (1.1.2, 1.1.3, 1.1.4), with $\theta^+ = \theta^- + y^-$.

3 Travelling waves

For the travelling wave analysis we replace x by $x + \mu t$, and the equations (2.2.1) and (2.2.6) by

$$Y_t = Y_{xx} - \mu Y_x, \quad x < s(t); \tag{3.3.1}$$

$$\Theta_t = \Theta_{xx} - \mu\Theta_x + \chi(f(\theta^+) - f(\Theta)), \quad x \neq s(t), \tag{3.3.2}$$

with a new meaning for $s(t)$ of course. This change does not affect the jump/boundary conditions (2.2.4). Recall that $\theta^+ = \theta^- + y^-$.

A travelling wave solution for given y^- and θ^- is a triple $(\mu, \theta(x), y(x))$ which solves

$$\begin{gathered} y''(x) - \mu y'(x) = 0, \quad x < 0; \\ \theta''(x) - \mu\theta'(x) + \chi(f(\theta^+) - f(\theta(x))) = 0, \quad x \neq 0; \\ y(-\infty) = y^-; \quad \theta(\pm\infty) = \theta^- + y^- = \theta^+; \\ y(0) = [\theta] = 0; \quad -y'(0) = -[\theta'] = F(\theta(0)) = \mu y^-, \end{gathered}$$

where the brackets denote the jump in $x = 0$. Keeping θ^- fixed we have y^- as one single control parameter.

3.1 Global travelling wave analysis

A travelling wave solution is completely determined by μ and $\theta^* = \theta(0)$, since $\theta = \theta(x)$ follows uniquely from solving

$$\theta'' - \mu\theta' + \chi(f(\theta^+) - f(\theta)) = 0, \quad x \neq 0; \quad \theta(\pm\infty) = \theta^+; \quad \theta(0) = \theta^*, \tag{3.3.3}$$

as we shall see below. The key point in the analysis below is that θ^* parametrises the solution set in the (y^-, μ)-plane.

Theorem 3.1 *Let $\theta^- > 0$ be fixed, let $F(\theta)$ be positive, smooth and increasing on an interval (θ_{ig}, ∞), $\theta_{ig} > \theta^-$, let $f(\theta)$ be smooth and increasing with $f(0) = 0$ and $f(\infty) = \infty$, and let $\chi > 0$ be fixed. Then there exists a smooth solution curve $\theta^* \to (y^-(\theta^*), \mu(\theta^*))$, $\theta^* \in (\theta_{ig}, \infty)$. Each point on the curve defines a travelling wave solution and there are no other travelling wave solutions.*

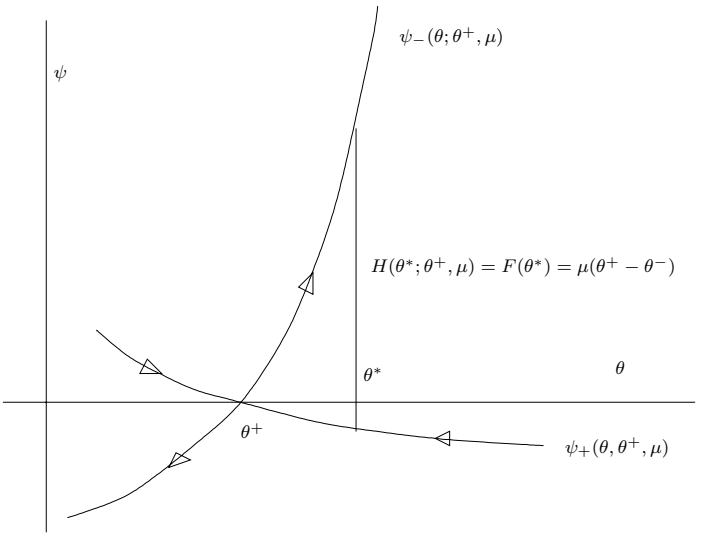

FIGURE 3. The phase plane for the proof of Theorem 3.1.

Remark 3.2 Since obviously

$$y(x) = y^-(1 - \exp(\mu x)),$$

the problem of finding travelling waves is reduced to solving (3.3.3) with

$$-[\theta'] = F(\theta(0)) = F(\theta^*) = \mu y^- = \mu(\theta^+ - \theta^-). \tag{3.3.4}$$

With y decoupled we consider from here on only the temperature profile. Bearing (1.1.1) in mind, θ^+ is then viewed as the control parameter, and the solution curve is represented as $\theta^* \to (\theta^+(\theta^*), \mu(\theta^*))$.

Proof Introducing $\psi = \theta'$ we study the (θ, ψ)-phase plane (Figure 3) which has a saddle point in $(\theta, \psi) = (\theta^+, 0)$. Let γ_- be the unique orbit emerging from this saddle having $\theta > \theta^+$ and $\psi > 0$ and γ_+ the orbit which goes into this saddle with $\theta > \theta^+$ and $\psi < 0$. In view of the conditions at infinity the two orbits γ_- and γ_+ represent the unknown profile $\theta(x)$ for, respectively, $x < 0$ and $x > 0$. We can write these orbits as graphs of functions of $\theta > \theta^+$:

$$\gamma_- : \quad \psi = \psi_-(\theta;\theta^+,\mu); \quad \gamma_+ : \quad \psi = \psi_+(\theta;\theta^+,\mu). \tag{3.3.5}$$

Then both ψ_- and ψ_+ satisfy, primes now denoting differentiation with respect to θ,

$$\psi'(\theta) = \mu + \chi\frac{f(\theta) - f(\theta^+)}{\psi(\theta)} \quad \theta > \theta^+, \tag{3.3.6}$$

with

$$\psi_-(\theta^+) = \psi_+(\theta^+) = 0, \tag{3.3.7}$$

and necessarily

$$\psi'_{\mp}(\theta^+) = \frac{1}{2}(\mu \pm \sqrt{\mu^2 + 4\chi f'(\theta^+)}). \tag{3.3.8}$$

Note that both ψ_- and ψ_+ are monotone (by inspection of the phase plane), defined for all $\theta > \theta^+$ (blow-up is impossible because ψ is in the denominator of the right hand side of (3.3.6)), but unbounded as $\theta \to \infty$ (since $f(\theta)$ is positive and unbounded). Moreover, we have

$$\psi_+(\theta)^2 < \psi_-(\theta)^2 \tag{3.3.9}$$

because

$$\psi_-(\theta)\psi'_-(\theta) - \psi_+(\theta)\psi'_+(\theta) = \mu(\psi_-(\theta) - \psi_+(\theta)) > 0.$$

Now define the function H by

$$H(\theta; \theta^+, \mu) = \psi_-(\theta; \theta^+, \mu) - \psi_+(\theta; \theta^+, \mu). \tag{3.3.10}$$

Then the travelling wave problem is equivalent to

$$H(\theta^*; \theta^+, \mu) = F(\theta^*) = \mu(\theta^+ - \theta^-), \tag{3.3.11}$$

which for $\mu > 0$ reduces further to

$$H\left(\theta^*; \theta^- + \frac{F(\theta^*)}{\mu}, \mu\right) = F(\theta^*). \tag{3.3.12}$$

Fixing $\theta^* > \theta_{ig}$ it is straightforward from (3.3.6) to see that we can make the left-hand side of (3.3.12) arbitrarily large by taking μ large. If we then decrease μ we can make

$$\theta^- + \frac{F(\theta^*)}{\mu}$$

increase to θ^* and thereby make the left-hand side of (3.3.12) as small as we want. Clearly, this implies that there exists a value of μ which solves (3.3.12).

Next we show that, for given θ^*, there is only one solution μ of (3.3.12) and that this solution varies smoothly with θ^*. Denoting the left hand side of (3.3.12) by $g(\mu, \theta^*)$, we note that by standard arguments $g(\mu, \theta^*)$ is smooth. Thus if we show that g_μ can never be zero, the solution is unique and varies smoothly with θ^*, in view of the implicit function theorem. To this end we need the derivatives of (3.3.10) with respect to μ and θ^+.

We first consider the μ-derivative. Let

$$\phi_\pm = \frac{d\psi_\pm}{d\mu}.$$

Then

$$\phi'_\pm(\theta) + \chi\frac{f(\theta) - f(\theta^+)}{\psi_\pm(\theta)^2}\phi_\pm(\theta) = 1, \quad \theta > \theta^+,$$

with

$$\phi_\pm(\theta^+) = 0,$$

and necessarily

$$\phi'_{\mp}(\theta^+) = \frac{1}{2}\left(1 \pm \frac{\mu}{\sqrt{\mu^2 + 4\chi f'(\theta^+)}}\right),$$

whence certainly ϕ_- is positive. For the difference $H_\mu = \phi_- - \phi_+$ we have the first order inhomogeneous linear differential equation

$$\begin{aligned} &H'_\mu(\theta) + \chi(f(\theta) - f(\theta^+))\frac{H_\mu(\theta)}{\psi_+(\theta)^2} \\ &\quad = \chi(f(\theta) - f(\theta^+))\phi_-(\theta)\left(\frac{1}{\psi_+(\theta)^2} - \frac{1}{\psi_-(\theta)^2}\right) > 0, \end{aligned}$$

(in view of (3.3.9)) with

$$H_\mu(\theta^+) = 0; \quad H'_\mu(\theta^+) = \frac{1}{\sqrt{\mu^2 + 4\chi f'(\theta^+)}} > 0,$$

so we may conclude that

$$H_\mu > 0. \tag{3.3.13}$$

Next we consider the θ^+-derivative, so now let

$$\phi_\pm = \frac{d\psi_\pm}{d\theta^+}.$$

Then

$$\phi'_\pm(\theta) + \chi\frac{f(\theta) - f(\theta^+)}{\psi_\pm(\theta)^2}\phi_\pm(\theta) = -\frac{\chi f'(\theta^+)}{\psi_\pm(\theta)}, \quad \theta > \theta^+,$$

with, by differentiating (3.3.7) and using (3.3.8),

$$\phi_\mp(\theta^+) = -\frac{1}{2}(\mu \pm \sqrt{\mu^2 + 4\chi f'(\theta^+)}),$$

whence certainly ϕ_- is negative and ϕ_+ positive. For the difference $H_{\theta^+} = \phi_- - \phi_+$ we have

$$\begin{aligned} &H'_{\theta^+}(\theta) + \chi(f(\theta) - f(\theta^+))\frac{H_{\theta^+}(\theta)}{\psi_+(\theta)^2} \\ &\quad = \chi(f(\theta) - f(\theta^+))\phi_-(\theta)\left(\frac{1}{\psi_+(\theta)^2} - \frac{1}{\psi_-(\theta)^2}\right) \\ &\qquad - \chi f'(\theta^+)\left(\frac{1}{\psi_-(\theta)} - \frac{1}{\psi_+(\theta)}\right) < 0, \end{aligned}$$

with

$$H_{\theta^+}(\theta^+) = -\sqrt{\mu^2 + 4\chi f'(\theta^+)} < 0.$$

We conclude that

$$H_{\theta^+} < 0. \tag{3.3.14}$$

Recalling that (3.3.12) rewrites as

$$H\left(\theta^*; \theta^- + \frac{F(\theta^*)}{\mu}, \mu\right) = g(\mu, \theta^*) = F(\theta^*),$$

(3.3.13,3.3.14) imply $g_\mu > 0$. This completes the proof of the existence and uniqueness of a smooth solution curve $\theta^* \to (\theta^+(\theta^*), \mu(\theta^*))$, or, equivalently, $\theta^* \to (y^-(\theta^*), \mu(\theta^*))$. Note that we really have a curve. Since $\mu(\theta^*)(\theta^+(\theta^*) - \theta^-) = F(\theta^*)$, the tangent vector is never zero. □

3.2 Bifurcation from the ignition temperature

In view of (3.3.11) and ignoring the y-component, we may think of $\mu = 0$ and $\theta^+ = \theta^* \leqslant \theta_{ig}$ as the trivial solution. With an abuse of language we refer to what happens at the end point $\mu = 0$, $\theta^+ = \theta_{ig}$ as bifurcation from the ignition temperature.

Theorem 3.3 *Suppose that the assumptions of Theorem 3.1 are satisfied and that F is also continuous in $\theta = \theta_{ig}$. Then $\mu(\theta^*) \to 0$ and $\theta^+(\theta^*) \to \theta_{ig}$ as $\theta^* \to \theta_{ig}$. Moreover, as $\theta \downarrow \theta_{ig}$,*

$$\theta^+(\theta^*) = \theta^* - \frac{F(\theta^*)}{2\sqrt{\chi f'(\theta_{ig})}} + o(F(\theta^*)); \quad \mu(\theta^*) = \frac{F(\theta^*)}{\theta_{ig} - \theta^-} + o(F(\theta^*)).$$

If $F'(\theta_{ig}^+)$ exists, the curve starts out to the left if $F'(\theta_{ig}^+) > 2\sqrt{\chi f'(\theta_{ig})}$ and to the right if $F'(\theta_{ig}^+) < 2\sqrt{\chi f'(\theta_{ig})}$.

Proof Since $F(\theta^*) \to 0$ as $\theta^* \downarrow \theta_{ig}$, it is easy to see that in the same limit $\mu(\theta^*) \to 0$. Otherwise (3.3.4) implies immediately that $\theta^+(\theta^*) \to \theta^-$. In view of $\theta^* \to \theta_{ig}$ and (3.3.6) the jump $-[\theta']$ then has to stay away from zero, because in (3.3.5) the monotonicity in μ implies $\psi_-(\theta; \theta^+, \mu) > \psi_-(\theta; \theta^+, 0)$. This contradicts $F(\theta^*) \to 0$.

From the definition of H in (3.3.10) it then also follows that $\theta^+(\theta^*) \to \theta_{ig}$, so we can consider the bifurcation of the curve from $\mu = 0$, $\theta^+ = \theta_{ig}$. We first consider the 'linear' case

$$f(\theta) = \theta,$$

for which (3.3.3) can be solved exactly to give

$$\theta(x) = \theta^+ + (\theta^* - \theta^+) \exp\left(\frac{x}{2}(\mu \pm \sqrt{\mu^2 + 4\chi})\right),$$

with a plus for $x < 0$ and a minus for $x > 0$. Thus, (3.3.4) becomes

$$(\theta^* - \theta^+)\sqrt{\mu^2 + 4\chi} = F(\theta^*) = \mu(\theta^+ - \theta^-).$$

Since $\mu(\theta^*) \to 0$ we conclude that

$$\theta^+(\theta^*) = \theta^* - \frac{F(\theta^*)}{2\sqrt{\chi}} + o(F(\theta^*)); \quad \mu(\theta^*) = \frac{F(\theta^*)}{\theta_{ig} - \theta^-} + o(F(\theta^*)),$$

as $\theta \downarrow \theta_{ig}$. It is easy to see that for nonlinear f the same conclusions hold with χ replaced by $\chi f'(\theta_{ig})$. This completes the proof. □

3.3 Heat loss parameter dependence and multiplicity

In this section, we discuss the limits $\chi \to 0$ and $\chi \to \infty$ and conclude that for small χ the behaviour illustrated in Figure 2 does indeed occur. If we follow the reasoning starting from (3.3.6) we see for $\mu > 0$ and $\chi = 0$ that $\psi_+(\theta) = 0$ and $\psi_-(\theta) = \mu(\theta - \theta^+)$, whence, in view of (3.3.11), $\theta^* = 2\theta^+ - \theta^-$. Thus in this limit the curve in Theorem 3.1/Remark 3.2 is given by

$$\theta^+ = \frac{\theta^* + \theta^-}{2}; \quad \mu = \frac{2F(\theta^*)}{\theta^* - \theta^-}, \tag{3.3.15}$$

but this only under the assumption that $\mu > 0$. Note that this curve starts at $\mu = 0$ and $\theta^+ = (\theta_{ig} + \theta^-)/2$, which is to the left of the end point of the solution curves for $\chi > 0$. For $\chi > 0$ but small we find by continuity a branch near (3.3.15) which, decreasing θ^*, has to turn around and go to this end point as $\theta^* \downarrow \theta_{ig}$. Since in fact (3.3.15) perturbs to a unique branch, the other branches must have $\mu \to 0$ as $\chi \to 0$ and therefore (in the same limit) $\theta^* = \theta_{ig}$. Depending on whether $F'(\theta_{ig}) > 0$ or $F'(\theta_{ig}) = 0$ there are then at least two and at least three branches, respectively.

If we consider the limit $\chi \to \infty$ it is easy to see from (3.3.6) and the subsequent formulas that for fixed θ^* necessarily $\theta^+ \to \theta^*$, because otherwise $H(\theta^*, \theta^+, \mu, \chi) = F(\theta^*)$ would blow up. Therefore we find in this limit that

$$\theta^+ = \theta^*; \quad \mu = \frac{F(\theta^*)}{\theta^* - \theta^-},$$

so that for large χ there is only one branch.

3.4 Large front temperatures

Theorem 3.1/Remark 3.2 provides us with a unique smooth solution curve $(\theta^+(\theta^*), \mu(\theta^*))$ parametrised by $\theta^* > \theta_{ig}$. To draw conclusions for the limit $\theta^* \to \infty$ we need to assume that F is bounded, which is of course true for the Arrhenius type reaction rate (3.3.20). We note though that in the physical context everything takes place in a θ^*- range where $F(\theta^*)$ is nowhere near being almost flat.

Theorem 3.4 *Suppose that the assumptions of Theorem 3.1 are satisfied and that $F(\theta)$ remains bounded as $\theta \to \infty$. Then eventually the curve $\theta^* \to (\theta^+(\theta^*), \mu(\theta^*))$ is moving to the right and downwards in the (θ^+, μ)-plane, with $\theta^+(\theta^*) \to \infty$ and $\mu(\theta^*) \to 0$ as $\theta^* \to \infty$.*

Proof By the same argument as in § 3.2, $\theta^+(\theta^*) \to \infty$ as $\theta^* \to \infty$, because otherwise the jump $-[\theta']$ becomes arbitrarily large. In view of $\mu(\theta^+ - \theta^-) = F(\theta^*)$, the other statements follow. □

3.5 Turning points

We recall from the proof of Theorem 3.1 and (3.3.11) that the solution curve has

$$H(\theta^*;\theta^+(\theta^*),\mu(\theta^*)) = F(\theta^*) = \mu(\theta^*)(\theta^+(\theta^*) - \theta^-), \tag{3.3.16}$$

where H is defined by (3.3.10).

Theorem 3.5 *Suppose that the assumptions of Theorem 3.1 are satisfied. Then*

$$\frac{d\theta^+}{d\theta^*} = 0 \quad \Longleftrightarrow \quad H_\mu = (F' - H')\frac{F}{\mu F'} \quad \Longrightarrow \quad \frac{d\mu}{d\theta^*} > 0, \tag{3.3.17}$$

and

$$\frac{d\mu}{d\theta^*} = 0 \quad \Longleftrightarrow \quad H_{\theta^+} = (F' - H')\frac{\mu}{F'} \quad \Longrightarrow \quad \frac{d\theta^+}{d\theta^*} > 0. \tag{3.3.18}$$

Note that only (3.3.17) *corresponds to a turning point in the sense of the explanation in the introduction.*

Proof The second equality in (3.3.16) implies that increasing θ^* the curve moves through the family of hyperbolas where $\mu(\theta^+ - \theta^-)$ is constant. In particular, the derivatives of $\mu(\theta^*)$ and $\theta^+(\theta^*)$ cannot be both nonpositive. Thus the only two possibilities for turning points are

$$\frac{d\theta^+}{d\theta^*} = 0; \quad \frac{d\mu}{d\theta^*} > 0,$$

and

$$\frac{d\theta^+}{d\theta^*} > 0; \quad \frac{d\mu}{d\theta^*} = 0.$$

From (3.3.16) we have

$$H_{\theta^+}\frac{d\theta^+}{d\theta^*} + H_\mu\frac{d\mu}{d\theta^*} = F'(\theta^*) - H'(\theta^*); \quad \mu\frac{d\theta^+}{d\theta^*} + (\theta^+ - \theta^-)\frac{d\mu}{d\theta^*} = F'(\theta^*),$$

whence

$$\frac{d\theta^+}{d\theta^*} = \frac{-(\frac{F}{\mu} - H_\mu)F' + \frac{H'F}{\mu}}{H_\mu\mu - H_{\theta^+}\frac{F}{\mu}}. \tag{3.3.19}$$

The denominator in (3.3.19) is positive so the numerator determines the sign and (3.3.17) follows. The proof of (3.3.18) is similar and omitted. □

Corollary 3.6 *In view of* (3.3.19)*, the critical value for* $F'(\theta^*)$ *is*

$$\frac{FH'}{F - \mu H_\mu} = \frac{HH'}{H - \mu H_\mu},$$

provided this quantity is positive. Otherwise the critical value is $+\infty$*. If* $F'(\theta^*)$ *is below (above) the critical value the solution curve moves to the right (left).*

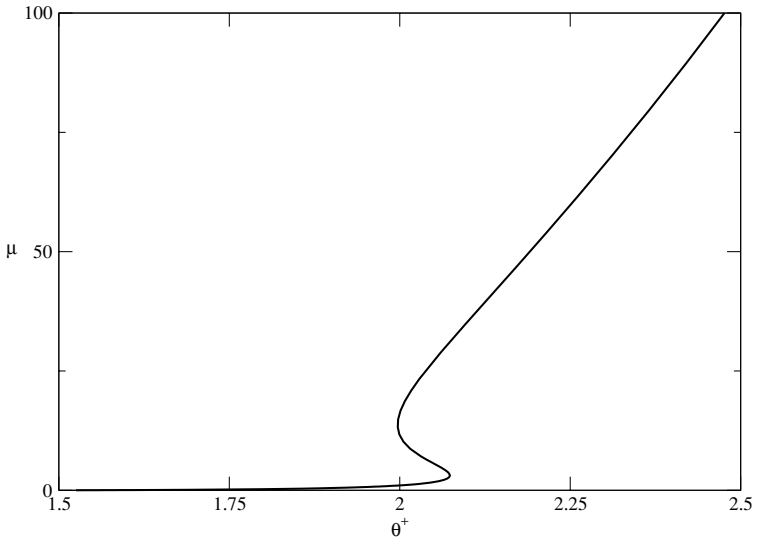

FIGURE 4. The solution diagram for $A = 10^5, \epsilon = 1/24, \alpha = 0.1, \chi = 1, \theta^- = 1$.

In what follows we shall understand turning points to be points where (3.3.17) holds. Depending on the higher order derivatives of H and F the solution curve in such a point may turn to the left or to the right, and, as we argue in Section 4, becomes, respectively, unstable or stable.

3.6 Numerics for the full problem

In this section, we show by means of numerical calculations that the full problem has a travelling wave solution diagram similar to the limit problem. We have used the continuation software AUTO (Doedel *et al.*, 1997) for ordinary differential equations to perform the numerics.

In line with the literature, we have done this for a reaction rate given by a simplified Arrhenius law, more precisely by

$$F(\theta^*) = A \exp\left(-\frac{1}{\epsilon\theta^*}\right), \tag{3.3.20}$$

where ϵ is a dimensionless inverse activation energy (small), and A is a (large) positive constant, the so-called pre-exponential factor. We checked that modifying this law with an ignition temperature leads to identical pictures (within the resolution of the eye). The solution curve shown in Figure 4 indicates that for large A and small ϵ a hysteresis effect can be observed. As for $\alpha = 0$, the curve is parametrised by θ^*.

For reaction rates without an ignition temperature the parametrised solution curve $\theta^* \to (Y^-(\theta^*), \mu(\theta^*))$ continues down to $\theta^* = \theta^-$, implying

$$\mu(\theta^*)y^-(\theta^*) \sim F(\theta^-), \quad \theta^* \downarrow \theta^-,$$

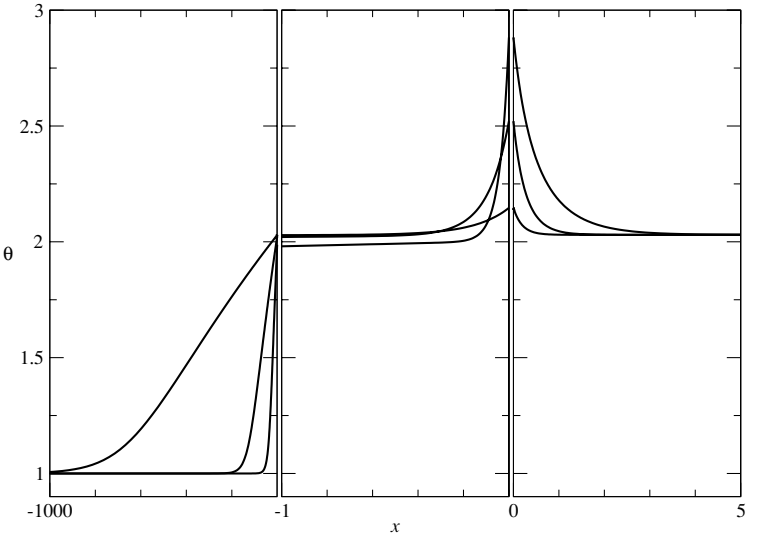

FIGURE 5. Three temperature profiles for $\theta^+ = 2.03$ in Figure 4. Notice the three different spatial scales.

whence $\mu(\theta^*) \to \infty$. Note though that in this limit $y^-(\theta^*) \to 0$ and the profiles become flat. The diagram in Figure 4 does not show this part of the curve, because it is hard to resolve numerically.

In Figure 5 we plot three temperature profiles corresponding to a fixed value of θ^+, two stable and one unstable. If we solve (3.3.3) for given μ subject only to

$$-[\theta'] = \mu(\theta^+ - \theta^-),$$

one easily shows that θ^* is uniquely determined as an increasing function of $\mu/\sqrt{\chi}$, which goes from θ^+ to $2\theta^+ - \theta^-$ as μ goes from zero to infinity (see also [7], where we showed for the full problem that θ^* is between θ^+ and $2\theta^+ - \theta^-$). In Figure 5 we see that the large stable solution with the higher speed has a temperature overshoot close to this upper bound, while the other two solutions, as well as the solution depicted in Figure 1, have a much smaller overshoot.

In Figure 6 we compare the solution diagram for small nonzero α with $\alpha = 0$, and we see that the reduced model indeed approximates the full problem for small α very well. In this figure we have plotted the renormalised wave speed $\frac{\mu}{\mu_{\text{ad}}}$, where the adiabatic wave speed (the wave speed in absence of radiation) is given by $\mu_{\text{ad}} = F(\theta^+)/y^-$. The figure thus confirms that radiation may significantly enhance the wave speed (cf. Joulin & Eudier, 1988).

4 Linearised stability analysis

In this section we apply the linearisation technique for FBPs with jump conditions (Brauner *et al.*, 2000), and compute the corresponding linearised system. Then we introduce

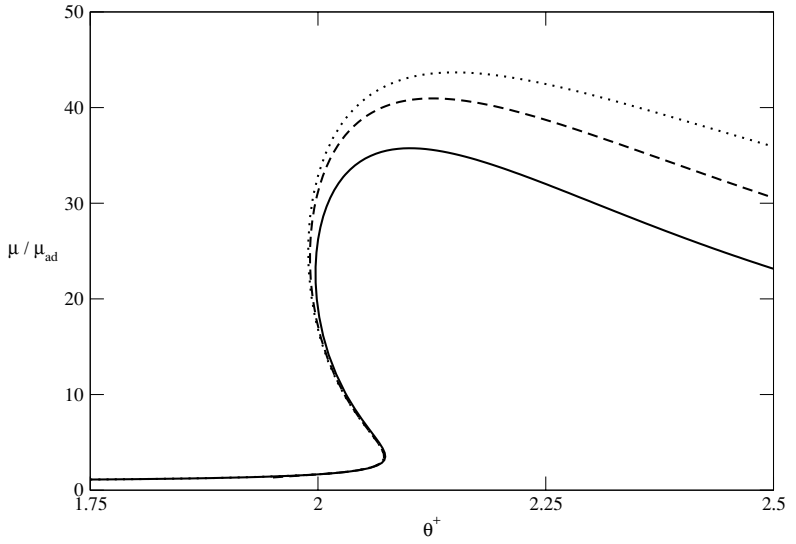

FIGURE 6. The solution diagram for $A = 10^5, \epsilon = 1/24, \chi = 1, \theta^- = 1$ with $\alpha = 0.1$ (solid), $\alpha = 0.05$ (dashed) and $\alpha = 0$ (dotted). The wave speed μ is normalised by the adiabatic wave speed μ_{ad}.

an Evans' function $D(\lambda)$ to characterise the spectrum and relate the behaviour of $D(\lambda)$ near $\lambda = 0$ to the turning point condition (3.3.17). Finally we give an explicit formula for $D(\lambda)$ when f is taken to be a linear function (i.e. $4 = 1$ in (1.1.5)).

4.1 The linearised equations

Starting from the travelling wave setting (3.3.1, 3.3.2), we introduce the new spatial variable

$$z = x - s(t),$$

and define $w(z,t)$ and $p(z,t)$ by

$$Y(x,t) = y(z) + s(t)y'(z) + w(z,t); \quad \Theta(x,t) = \theta(z) + s(t)\theta'(z) + p(z,t).$$

This fixes the free boundary and leads to, with dots denoting time derivatives,

$$w_t - w_{zz} + \mu w_z = \dot{s}w_z + \dot{s}sy'', \quad z < 0;$$
$$p_t - p_{zz} + \mu p_z + \chi f'(\theta)p = \dot{s}p_z + \dot{s}s\theta'' + q(p,s), \quad z \neq 0,$$

with jump/boundary conditions

$$w = [p];$$

$$w_z = [p_z] = \mu[p] + \frac{F'(\theta(0))}{F(\theta(0))}(\theta'(0^+)p(0^-) - \theta'(0^-)p(0^+)) + Q^{\pm}(p,s)$$

in $z = 0$. Here

$$q(p,s) = \chi f(\theta) + \chi f'(\theta)(s\theta' + p) - \chi f(\theta + s\theta' + p),$$
$$Q^{\pm}(p,s) = F(\theta(0)) + F'(\theta(0))(s\theta'(0^{\pm}) + p(0^{\pm})) - F(\theta(0) + s\theta'(0^{\pm}) + p(0^{\pm})),$$

which are both at least quadratic in p and s (the assumption that we are close to the travelling wave means that s, w and p are small). The free boundary terms s and $\dot{s}$ are eliminated using

$$w(0) = sF(\theta(0)); \quad \dot{s} = \frac{w_{zz}(0) - \mu w_z(0)}{F(\theta(0)) - w_z(0) + \mu w(0)},$$

and the linearised evolution equations for w and p are

$$w_t = w_{zz} - \mu w_z, \quad z < 0; \tag{4.4.1}$$
$$p_t = p_{zz} - \mu p_z - \chi f'(\theta)p, \quad z \neq 0, \tag{4.4.2}$$

with (linearised) jump/boundary conditions

$$w = [p]; \quad w_z = [p_z] = \mu[p] + \frac{F'(\theta^*)}{F(\theta^*)}(\theta'(0^+)p(0^-) - \theta'(0^-)p(0^+)). \tag{4.4.3}$$

4.2 The Evans function

The eigenvalue problem for the linearised problem (4.4.1,4.4.2,4.4.3) reads

$$w'' - \mu w' = \lambda w, \quad x < 0; \quad p'' - \mu p' - \chi f'(\theta)p = \lambda p, \quad x \neq 0, \tag{4.4.4}$$

with jump/boundary conditions

$$w(0) = [p]; \quad w'(0) = [p']; \quad w'(0) - \mu w(0) = \frac{F'(\theta(0))}{F(\theta(0))}(\theta'(0^+)p(0^-) - \theta'(0^-)p(0^+)). \tag{4.4.5}$$

We look for solutions which are well behaved (e.g. bounded) as $x \to \pm\infty$. The precise definition of 'well behaved' depends upon the choice of function spaces, which is not the issue here. Eigenfunctions may be sought in the form

$$w(x) = Aw(x;\lambda);$$
$$p(x) = B^{-}p(x;\lambda) \quad (x < 0);$$
$$p(x) = = B^{+}p(x;\lambda) \quad (x > 0),$$

where $w(x;\lambda)$ and $p(x;\lambda)$ are solutions of (4.4.4) with (exponential) decay rates determined by the characteristic roots of the limit equations at infinity. These two roots are two 2-valued complex analytic functions

$$\lambda \to \frac{1}{2}(\mu + \sqrt{\mu^2 + 4\lambda}), \tag{4.4.6}$$

and

$$\lambda \to \frac{1}{2}(\mu + \sqrt{\mu^2 + 4\chi f'(\theta^+) + 4\lambda}). \tag{4.4.7}$$

We normalise $w(x;\lambda)$ and $p(x;\lambda)$ by asking that $w(0;\lambda) = p(0;\lambda) = 1$. In general $p'(\cdot;\lambda)$ will have a jump in $x = 0$.

One can show that as long as λ does not cross the cuts for (4.4.6) and (4.4.7) at the negative real axis in the complex plane, the functions $w(x;\lambda)$ and $p(x;\lambda)$ exist and are unique. In the case that f is linear this is immediate from the explicit exponential formulas for $w(x;\lambda)$ and $p(x;\lambda)$.

The conditions (4.4.5) give three equations for A, B^- and B^+, so that a determinant has to be zero to have an eigenfunction. We derive this condition in the form $D(\lambda) = 0$, and refer to $D(\lambda)$ as the Evans function for (4.4.4,4.4.5).

It is easily seen that A must be nonzero. Normalising we find from the first jump condition in (4.4.5) that

$$A = 1; \quad B^- = -B; \quad B^+ = 1 - B,$$

from the second that

$$B(p'(0^-;\lambda) - p'(0^+;\lambda)) = \frac{1}{2}(\mu + \sqrt{\mu^2 + 4\lambda}) - p'(0^+;\lambda), \tag{4.4.8}$$

and from the last that

$$BF'(\theta^*) = \frac{1}{2}(-\mu + \sqrt{\mu^2 + 4\lambda}) + \frac{F'(\theta^*)}{F(\theta^*)}\theta'(0^-). \tag{4.4.9}$$

The two equations (4.4.8) and (4.4.9) allow a (unique) solution for B if and only if

$$\begin{aligned} D(\lambda) &= (p'(0^-;\lambda) - p'(0^+;\lambda))\left(\frac{1}{F'(\theta^*)}\frac{-\mu + \sqrt{\mu^2 + 4\lambda}}{2} + \frac{\theta'(0^-)}{F(\theta^*)}\right) \\ &\quad + p'(0^+;\lambda) - \frac{\mu + \sqrt{\mu^2 + 4\lambda}}{2} \\ &= (p'(0^-;\lambda) - p'(0^+;\lambda))\left(\frac{1}{F'(\theta^*)}\frac{-\mu + \sqrt{\mu^2 + 4\lambda}}{2} + \frac{\theta'(0^+)}{F(\theta^*)}\right) \\ &\quad + p'(0^-;\lambda) - \frac{\mu + \sqrt{\mu^2 + 4\lambda}}{2} \qquad (4.4.10) \\ &= 0. \qquad (4.4.11) \end{aligned}$$

One readily verifies that $D(0) = 0$ and that the corresponding eigenfunction is

$$\phi = \begin{pmatrix} y' \\ \theta' \end{pmatrix}.$$

Another calculation then gives

$$D'(0) = \frac{1}{F(\theta^*)}\left(\frac{\int_{-\infty}^{0} \frac{\theta'(s)^2}{\exp(\mu s)} ds}{\theta'(0^-)} + \frac{\int_{0}^{\infty} \frac{\theta'(s)^2}{\exp(\mu s)} ds}{\theta'(0^+)}\right) - \frac{F'(\theta^*) + \chi(f(\theta^*) - f(\theta^+))[\frac{1}{\theta'}]}{\mu F'(\theta^*)}.$$

To determine the connection with turning points, we note that if we apply the implicit function theorem to the travelling wave problem without going to the phase plane, we find from

$$\theta_\mu'' - \mu\theta_\mu' - \chi f'(\theta)\theta_\mu = \theta'; \quad \theta_\mu(0) = 0$$

that

$$\theta_\mu(x) = \theta'(x)E_\pm(x),$$

where

$$E_\pm(x) = \int_0^x \frac{\exp(\mu y)}{\theta'(y)^2} \int_{\pm\infty}^y \frac{\theta'(s)^2}{\exp(\mu s)}\, ds\, dy,$$

with a plus for $x > 0$ and a minus for $x < 0$. Thus, since $H = -[\theta']$ by (3.3.10),

$$H_\mu = \frac{1}{\theta'(0^-)} \int_{-\infty}^0 \frac{\theta'(s)^2}{\exp(\mu s)}\, ds + \frac{1}{\theta'(0^+)} \int_0^\infty \frac{\theta'(s)^2}{\exp(\mu s)}\, ds,$$

and the turning point condition (3.3.17) is equivalent to

$$\begin{aligned} &\frac{1}{\theta'(0^-)} \int_{-\infty}^0 \frac{\theta'(s)^2}{\exp(\mu s)}\, ds + \frac{1}{\theta'(0^+)} \int_0^\infty \frac{\theta'(s)^2}{\exp(\mu s)}\, ds \\ &\quad - \frac{F(\theta^*)}{\mu F'(\theta^*)} \left(F'(\theta^*) + \chi(f(\theta^*) - f(\theta^+)) \left[\frac{1}{\theta'} \right] \right) = 0, \end{aligned} \tag{4.4.12}$$

which in turn is equivalent to $D'(0) = 0$, completely consistent with Kapitula (1999). Also, it follows directly from (3.3.19) that the sign of $D'(0)$ coincides with $d\theta^+/d\theta^*$. As an immediate consequence we have

Theorem 4.1 *Suppose $D''(0) > 0$ in a point where $d\theta^+/d\theta^* = 0$. Moving along the solution curve a positive (negative) eigenvalue goes through zero if $d\theta^+/d\theta^*$ becomes negative (positive)*

We spare the reader the formula for $D''(0)$. In the linear case discussed below, it is always positive in turning points.

4.3 Numerical investigation of the Evans function

In this section we compare numerically the Evans functions for $n = 4$ and $n = 1$. For $n = 1$ the calculations can be checked and substantiated analytically (see § 4.4. As in § 3.6, the numerical calculations are performed using AUTO.

In view of (4.4.10) we rewrite the Evans' function in the form

$$\frac{F'(\theta^*)D(\lambda)}{\mu^2 + 4\lambda} = D_0(\lambda) - D_1(\lambda)F'(\theta^*).$$

The factor $\mu^2 + 4\lambda$ ensures that the limit of $D_0(\lambda)$ as $\lambda \to \infty$ is well defined, while no new zeros or poles are introduced away from the branch point $\lambda = -\mu^2/4$. Here we interpret $F'(\theta^*)$ as a parameter that can be varied while the travelling wave solution $\theta(x)$ is kept fixed (i.e. $F(\theta^*)$ is kept fixed), as already mentioned in the introduction.

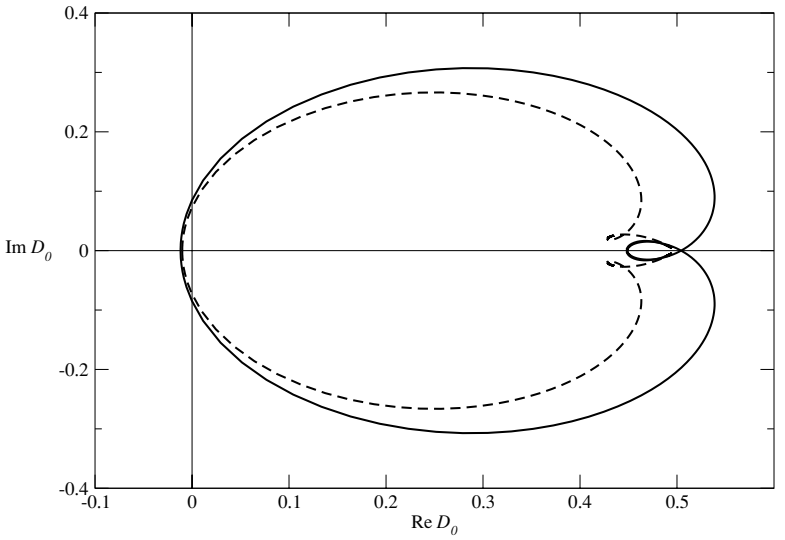

FIGURE 7. The image of $\ell = \{-0.1 + it \,|\, t \in \mathbb{R}\}$ under D_0 for $n = 1$ (dashed) and $n = 4$ (solid). The parameter values are $\theta^+ = 2$, $\theta_- = 1$, $\mu = 5$, and $\chi = 1$ ($n = 4$) and $\chi = 32$ ($n = 1$).

We calculate $D_0(\lambda)$ and $D_1(\lambda)$ on a vertical line

$$\ell = \{\lambda = -a + it \,|\, t \in \mathbb{R}\}$$

for some small $a > 0$. The idea is to close this curve at infinity so that it represents a contour around $\Omega = \{z \in \mathbb{C} \,|\, \mathrm{Re}\, z > -a\}$, which contains the right half plane.

Our approach is the following. We start at $F' = 0$, for which, as we will see, there is exactly one zero of $D(\lambda)$ in Ω, namely $\lambda = 0$ (due to translation invariance). We then monitor what happens on ℓ as F' increases. Clearly, a zero of $D(\lambda)$ crosses ℓ on the real axis when $F' = D_0(-a)/D_1(-a)$, provided this is positive. If another zero of $D(\lambda)$ crosses ℓ then $D_0(-a+it)/D_1(-a+it)$ has to be *real* for some $t \neq 0$. We shall see that this does not happen, i.e. for any $F' > 0$ there will be at most two zeros of $D(\lambda)$ in Ω, one at $\lambda = 0$ and one that crosses zero at $F' = F_c = \lim_{x \to 0} \frac{D_0(x)}{D_1(x)}$. This implies that for $F' < F_c'$ the wave is stable, while it is unstable for $F' > F_c'$.

We note that we take different values of χ for $n = 1$ and $n = 4$ so that the linear case $n = 1$ can be viewed as an approximation of the nonlinear case $n = 4$. To be more precise, linearising $\chi\theta^4$ around $\theta = \theta^+ = 2$ (which is an easy, albeit low, choice), we take a χ to be 32 times larger for $n = 1$ compared to $n = 4$. Indeed, the pictures for $n = 1$ and $n = 4$ turn out to be similar when this simple choice is made.

The outcome of the numerical calculations is presented in Figures 7 and 8. As explained above we start at $F' = 0$ where $D(\lambda) = D_0(\lambda)$. The image $D_0(\ell)$ is shown in Figure 7, where we have chosen $a = 0.1$. When one closes the contour, for both $n = 1$ and $n = 4$ the image winds around 0 exactly once, implying that there is exactly one zero of $D_0(\lambda)$ in Ω, namely $\lambda = 0$. Next, in Figure 8 we have depicted the image $\frac{D_0}{D_1}(\ell)$. For both $n = 1$

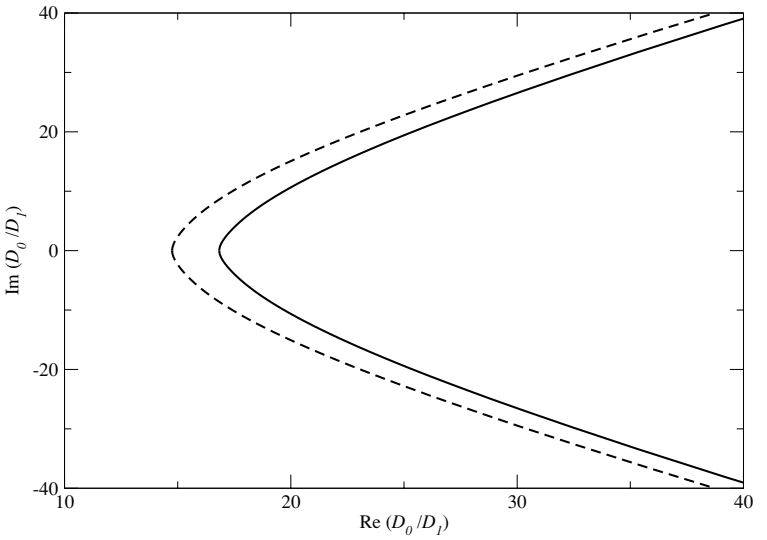

FIGURE 8. The image of ℓ under D_0/D_1 for $n = 1$ (dashed) and $n = 4$ (solid). The parameter values are the same as in Figure 7.

and $n = 4$ it crosses the real axis exactly once, implying that only one zero of $D(\lambda)$ crosses ℓ as F' is increased, and the conclusions drawn above about the stability hold.

4.4 The 'linear' problem

Replacing $f(\theta)$ by

$$f(\theta) = \theta,$$

we can almost solve the travelling wave problem in closed form. We have

$$\theta(x) = \theta^+ + (\theta^* - \theta^+)\exp\left(\frac{x}{2}(\mu \mp \sqrt{\mu^2 + 4\chi})\right),$$

$$\theta'(0^\pm) = (\theta^* - \theta^+)\frac{1}{2}(\mu \mp \sqrt{\mu^2 + 4\chi}),$$

and

$$F(\theta^*) = (\theta^* - \theta^+)\sqrt{\mu^2 + 4\chi}.$$

Slightly changing the definition of D, we obtain

$$\begin{aligned}\tilde{D}(\lambda) &= \frac{2F'(\theta^*)D(\lambda)}{\sqrt{\mu^2 + 4\chi + 4\lambda}} \\ &= -\mu + \sqrt{\mu^2 + 4\lambda} - F'(\theta^*)\left(\sqrt{\frac{\mu^2 + 4\lambda}{\mu^2 + 4\chi + 4\lambda}} - \frac{\mu}{\sqrt{\mu^2 + 4\chi}}\right),\end{aligned}$$

and we can completely solve the equation $D(\lambda) = 0$. Setting

$$4\lambda = \mu^2 z, \quad 4\chi = \mu^2 \omega \quad F'(\theta^*) = \mu\delta,$$

the equation $D(\lambda) = 0$ transforms in

$$D(z) = -1 + \sqrt{1+z} - \delta\left(\sqrt{\frac{1+z}{1+\omega+z}} - \frac{1}{\sqrt{1+\omega}}\right) = 0.$$

Fix $\omega > 0$. Taking δ large we see there are two real roots: $z = 0$ and a large positive root. Decreasing δ we hit the value $\delta = (1+\omega)^{3/2}/\omega$ where the positive root passes through zero and becomes negative. Decreasing δ further the negative root disappears in the branch point $z = -1$ for $\delta = \sqrt{1+\omega}$. For δ smaller there are no real roots except the origin.

Now take $\omega = 0$. Then the only (complex root) is zero. Making ω positive the only way complex roots can appear is as double real roots. But this can only be in $z = 0$ where $D(0) = 0$ and $D'(0) = 0$ implies $D''(0) > 0$, making it impossible for the roots to become complex.

Thus the picture in the 'linear' case is complete. It is only the size of $F'(\theta^*)$ which decides the stability and whether the solution curve moves to the right.

5 Conclusions

We have presented a simple model for combustion and radiation and we have shown that it captures surprisingly well the phenomena observed in the combustion literature. Thus the results in this paper are a revealing first step towards a full understanding of the complete problem, i.e. general α, β, Le, and exponent 4 in (1.1.5). The limit problem discussed here seems to be the first free boundary problem in which turning points are described in terms of an Evans function derived for the FBP itself, which motivates further study in this direction. The solution picture in this paper is reminiscent of that of the FitzHugh-Nagumo system – see Smoller (1994), where in the bifurcation diagram the slow and the fast pulse come together in a turning point.

We emphasise that our stability analysis and the relation with the role of turning points in the travelling wave diagram is for Le = 1. Varying Le the travelling wave analysis remains the same, but stability properties change. The limit problem studied in this paper, despite its simplicity, has a surprisingly rich structure, with turning points, Hopf bifurcations and (in more dimensions) cellular instabilities. The latter two are well established in similar problems with a trivial travelling wave diagram diagram such as the model without radiation (see also Balmforth *et al.* (1999), Bayliss *et al.* (1989), Alabau & Lunardi (1992), Brauner & Lunardi (2000) and Lorenzi & Lunardi (2003)). In a future work we shall examine the nearly equidiffusional setting where Le is coupled to the activation energy.

Finally, we observe that in the transition from the full model with α and β to our limit model, the outer layer on the left in front of the preheating zone disappears. In fact the full model can also be linearised around a travelling wave, but the spectral analysis is far more complicated (see also Buckmaster & Jackson (1994)). The Evans function has to be

constructed using exponents solving a quartic equation, one of which crosses zero as λ crosses zero. This will be work for the future.

Acknowledgements

We thank Luca Lorenzi for his corrections and the referee for his suggestions. This work is supported by a CNRS/NWO grant, the TMR network Nonlinear Parabolic Partial Differential Equations: Methods And Applications, ERBFMRXCT980201 and by RTN network Fronts-Singularities, HPRN-CT-2002-00274.

References

[1] Alabau, F. & Lunardi, A. (1992) Behavior near the travelling wave solution of a free boundary system in combustion theory. *Dynam. Systems Appl.* **1**, 391–417.

[2] Balmforth, N. J., Craster, R. V. & Malham, S. J. A. (1999) Unsteady fronts in an autocatalytic system. *R. Soc. Lond. Proc. Ser. A Math. Phys. Eng. Sci.* **455**, 1401–1433.

[3] Bayliss, A., Matkowski, B. J. & Minkoff, M. (1989) Period doubling gained, period doubling lost. *SIAM J. Appl. Math.* **49**, 1047–1063.

[4] Blouquin, R. (1996) *Contribution à l'étude théorique des interactions entre combustion et rayonnement*. PhD thesis, Université de Poitiers.

[5] Blouquin, R., Joulin, G. & Merhari, Y. (1997) Combustion regimes of particle-laden gaseous flames, influences of radiation, molecular transports, kinetic-quenching, stoichiometry. *Combust. Theory*, **1**, 217–242.

[6] Brauner, C.-M., Hulshof, J. & Lunardi, A. (2000) A general approach to stability in free boundary problems. *J. Diff. Eqns.* **164**, 16–48.

[7] Brauner, C.-M., Hulshof, J. & Ripoll, J.-F. (2001) Existence of travelling wave solutions in a combustion-radiation model. *Discrete and Continuous Dynamical Systems* **1**, 193–208.

[8] Brauner, C.-M. & Lunardi, A. (2000) Instabilities in a two-dimensional combustion model with free boundary. *Arch. Rat. Mech. Anal.* **154**, 157–182.

[9] Buckmaster, J. & Jackson, T. L. (1994) The effects of radiation on the thermal-diffusive stability boundaries of premixed flames. *Combust. Sci. and Tech.* **103**, 299–313.

[10] Buckmaster, J. D. & Ludford, G. S. S. (1982) *Theory of Laminar Flames.* Cambridge University Press.

[11] Doedel, E. J., Champneys, A. R., Fairgrieve, T. F., Kuznetsov, Y. A., Sandstede, B. & Wang, X. (1997) *AUTO97, continuation and bifurcation software for ordinary differential equations (with HomCont)*. Available by anonymous ftp from `ftp.cs.concordia.ca`, directory `pub/doedel/auto`.

[12] Dubroca, B. & Feugeas, J.-L. (1999) Etude théorique et numérique d'une hiérarchie de modèles aux moments pour le transfert radiatif. *C. R. Acad. Sci. Paris*, **329**, 915–920.

[13] Evans, J. W. (1975) Nerve axon equations. iv. the stable and the unstable impulse. *Indiana Univ. Math. J.* **25**, 1169–1190.

[14] Fife, P. C. (1998) *Dynamics of Internal Layers and Diffusive Interfaces.* SIAM.

[15] Joulin, G. & Eudier, M. (1988) Radiation-dominated propagation and extinction of slow, particle-laden gaseous flames. *22nd Int. Symp. on Combustion*, pp. 1579–1585.

[16] Kapitula, T. (1999) The Evans function and generalized Melnikov integrals. *SIAM J. Math. Anal.* **30**, 273–297.

[17] Levermore, C. D. (1996) Moments closure hierarchies for kinetic theories. *J. Stat. Phys.* **83**, 1021–1065.

[18] Lorenzi, L. & Lunardi, A. (2003) Stability in a two-dimensional free boundary combustion model. *Nonlinear Anal.* **53**, 227–276.

[19] Sivashinsky, G. I. (1977) Diffusional-thermal theory of cellular flames. *Comb. Sci. Tech.* **15**, 137–146.
[20] Smoller, J. (1994) *Shock Waves and Reaction-Diffusion Equations (2nd edition)*. Springer-Verlag.
[21] Terman, D. (1990) Stability of planar wave solutions to a combustion model. *SIAM J. Math. Anal.* **21**, 1139–1171.
[22] Williams, F. A. (1985) *Combustion Theory*. Perseus Books.